



Recent developments on ZnO films for acoustic wave based bio-sensing and microfluidic applications: a review

Y.Q. Fu^{a,b,*}, J.K. Luo^{b,c}, X.Y. Du^b, A.J. Flewitt^b, Y. Li^d, G.H. Markx^a, A.J. Walton^d, W.I. Milne^b

^a School of Engineering and Physical Sciences, Heriot Watt University, Edinburgh, EH14 4AS, UK

^b Department of Engineering, University of Cambridge, JJ Thomson Avenue, CB3 0FA, UK

^c Centre for Material Research and Innovation, University of Bolton, Deane Road, Bolton, BL3 5AB, UK

^d Scottish Microelectronics Centre, School of Engineering, University of Edinburgh, Edinburgh, EH10 7AT, UK

ARTICLE INFO

Article history:

Received 8 June 2009

Received in revised form 8 September 2009

Accepted 2 October 2009

Available online 10 November 2009

Keywords:

ZnO

Film

Biosensor

Microfluidics

SAW

FBAR

Lab on chip

ABSTRACT

Recent developments on the preparation and application of ZnO films for acoustic wave-based microfluidics and biosensors are reviewed in this paper. High quality and strongly textured ZnO thin films can be prepared using many technologies, among which RF magnetron sputtering is most commonly used. This paper reviews the deposition of ZnO film and summarizes the factors influencing the microstructure, texture and piezoelectric properties of deposited ZnO films. ZnO acoustic wave devices can be successfully used as biosensors, based on the biomolecule recognition using highly sensitive shear horizontal and Love-wave surface acoustic waves, as well as film bulk acoustic resonator devices. The acoustic wave generated on the ZnO acoustic devices can induce significant acoustic streaming, small scale fluid mixing, pumping, ejection and atomization, depending on the wave mode, amplitude and surface condition. The potential to fabricate an integrated lab-on-a-chip diagnostic system based on these ZnO acoustic wave technologies is also discussed.

© 2009 Elsevier B.V. All rights reserved.

1. Introduction

Acoustic wave technology and devices have been in commercial use (such as communications, automotive and environmental sensing) for more than 60 years [1,2]. When an alternating electric field is applied to an interdigital transducer (IDT) on a piezoelectric material, a mechanical wave can be generated and propagates into the material perpendicular to the surface into the bulk (bulk acoustic wave, BAW) or on the surface of the material (surface acoustic wave, SAW) through a piezoelectric effect, either in a Rayleigh mode (vertical and surface normal) or as a shear wave (horizontal in-plane) [3]. Table 1 lists some common acoustic wave modes and related sensors. The most commonly used bulk acoustic wave device is the quartz crystal microbalance (QCM), which is generally made of quartz sandwiched between two electrodes. A surface acoustic wave propagating within a thin surface layer, which has a lower acoustic velocity than that of the piezoelectric substrate, is called a Love wave. Love-wave devices are typically operated in the shear horizontal (SH) wave mode. A wave propagating in a thin plate with a thickness much less than the acoustic wave-

length is called a flexural plate wave or Lamb wave [4]. This paper first highlights acoustic wave-based microfluidics and biosensor technology before discussing the ZnO based ones. The following section reviews the deposition of ZnO film and summarizes the factors influencing the microstructure, texture and piezoelectric properties of deposited ZnO films. Bio-sensing and microfluidics applications based on the ZnO acoustic wave devices are reviewed. The potential to fabricate an integrated lab-on-a-chip diagnostic system based on these ZnO acoustic wave technologies is also discussed.

2. Acoustic wave bio-sensors and microfluidics

2.1. Acoustic wave biosensors

Most acoustic wave devices can be used as sensors because they are sensitive to mechanical, chemical, or electrical perturbations on the surface of the device [5,6]. Acoustic wave sensors have the advantage that they are versatile, sensitive, and reliable. They can detect not only mass/density changes, but also viscosity, wave functions, elastic modulus, conductivity and dielectric properties and have wide applications in monitoring of pressure, moisture, temperature, force, acceleration, shock, viscosity, flow, pH levels, ionic contaminants, odour, radiation and electric fields [7,8]. Recently,

* Corresponding author at: School of Engineering and Physical Sciences, Heriot Watt University, Edinburgh, EH14 4AS, UK.

E-mail address: R.Y.Fu@hw.ac.uk (Y.Q. Fu).

Table 1
Comparison of different acoustic wave microsensors.

Microsensor	QCM	Rayleigh SAW	SH-SAW	Flexural plate wave (FPW) Lamb Wave	Love wave	Film bulk acoustic wave (FBAR) Bulk wave
Mode	Thickness shear bulk mode	Rayleigh wave	Shear wave		SH-SAW	
Gas	✓	✓	✓	✓	✓	✓
Liquid	✓✓	×	✓✓	✓	✓✓	✓
Normal frequency	5–20 MHz	20–500 MHz		kHz to lower MHz		>GHz
Sensitivity (cm ² /g)	10–100	100–1000	10–500	100–1000	20–2000	1,000–10,000
Example	AT-cut quartz	ST-cut Quartz 120 °C LiNbO ₃	36YX LiTaO ₃ ST-cut quartz ZX-LiNbO ₃	Si ₃ N ₄ /ZnO membrane	SiO ₂ /ST-Quartz, ZnO/LiTaO ₃	ZnO and AlN membrane

there has been an increasing interest in acoustic wave based biosensors to detect the traces of biomolecules (biomarkers) such as DNA, proteins (enzymes, antibodies, and receptors), cells and tissue (microorganisms, animal and plant cells, cancer cells etc.), biochemical substances or viruses [9–11]. By detecting the traces of associated molecules, it is possible to diagnose diseases and genetic disorders, prevent potential bioattachment, and monitor the spread of viruses and pandemics [12–14]. Compared with some common bio-sensing technologies, such as surface plasmon resonance (SPR), optical fibres, and sensors based on field effect transistors or cantilever-based detectors, acoustic wave based technologies have the combined advantages of simple operation (electrical signal), high sensitivity, small size, low cost, and no need for bulky optical detection systems [15].

The most commonly reported acoustic wave based biosensor is the QCM [16], which can be operated in a liquid environment using a thickness shear mode. Problems associated with QCM biosensors include: (1) low mass detection limit due to the low operating frequency in the range of 5–20 MHz and large base-mass; (2) a thick substrate (0.5–1 mm) and large surface area (>1 cm²) which is not easily scalable.

Since the SAW based biosensors have their acoustic energy confined in the surface layer of about one wave length, the base-mass of the active layer is about one order of magnitude smaller than that of the QCM. Thus the sensitivity of the SAW devices increases dramatically compared with that of the QCM (see Table 1). The longitudinal or Rayleigh mode SAW device has a substantial surface-normal displacement that easily dissipates the acoustic wave energy into the liquid, leading to excessive damping, and hence poor sensitivity and noise. Waves in a SH-SAW device propagate in a shear horizontal mode, and do not easily radiate acoustic energy into the liquid [17,18] and thus maintain a high sensitivity in liquids. Therefore SH-SAW devices are particularly well suited for bio-detection, especially for “real-time” monitoring. In most cases, Love-wave devices operate in the SH wave mode with the acoustic energy trapped within a thin guiding layer (typically submicrometer). This enhances the detection sensitivity by more than two orders of magnitude as compared with a SAW device owing to a much-reduced base-mass [19,20]. In addition, the wave guide layer in the Love mode biosensor can also protect and insulate the IDT from the liquid media which might otherwise be detrimental to the electrode. Therefore, they are frequently utilized to perform bio-sensing in liquid conditions [21–23].

In a similar manner to a SAW device, Lamb wave devices on a membrane structure have been used for bio-sensing in liquids [24]. The wave velocity generated in the FPW or Lamb wave is much smaller than those in liquids, which minimizes the dissipation of wave energy into the liquid. The detection mechanism is based on the relative change in magnitude induced by the perturbation on the membrane, not on the resonant frequency shift. Therefore the sensitivity of a Lamb wave device increases as the

membrane thickness becomes thinner [25,26]. The main drawback of the Lamb wave biosensor is that there is a practical limitation in film thickness as the thin film becomes more fragile.

A newly emerged but promising acoustic wave device for high-sensitivity bio-detection is the film bulk acoustic resonator (FBAR) device. Similar to the structure of a QCM, a FBAR device consists of a submicrometer thick piezoelectric film membrane sandwiched between two metallic layer electrodes [27]. Owing to the much-reduced thickness, the FBAR device operates at a high frequency, up to a few GHz (see Table 1). The frequency shift Δf due to mass loading Δm of an acoustic wave device is described by [28]

$$\Delta f = \frac{2\Delta m f_0^2}{A\sqrt{\rho\mu}} \quad (1)$$

where A , ρ , μ and f_0 are the area, density, shear modulus and intrinsic resonant frequency, respectively. Due to the much-reduced base-mass and high operation frequency, the attachment of a small target mass can cause a large frequency shift—typically a few MHz. This makes the signal easily detected using simple electronic circuitry. The advantages of the FBAR devices include: (1) the ability to fabricate the device using standard CMOS processing and materials allowing integration with CMOS control circuitry; (2) the size and volume can be significantly reduced. These features together with the intrinsic high sensitivity make the FBAR technology ideal for real time diagnostic biosensor arrays, which are highly sensitive, providing quantitative results at a competitive cost.

2.2. Acoustic wave-based microfluidics

Microfluidic (liquid samples and reagents) manipulation, mixing and biochemical reaction at the microscale are extremely difficult due to the low Reynolds number flow conditions [29]. Acoustic wave technologies are particularly well suited for mixing and as a result are attractive options for microfluidics applications [30]. Taking SAW devices as one example, Rayleigh-based SAW

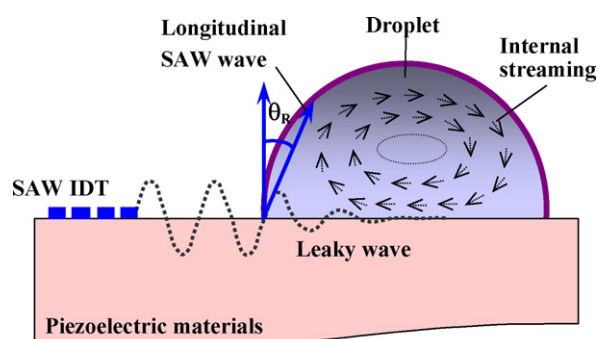


Fig. 1. Interaction between propagating surface acoustic wave and a liquid droplet causing acoustic streaming inside droplet.

Table 2
Comparison of common piezoelectric materials.

Materials	ZnO	AlN	PZT	Quartz	128° cut LiNbO ₃	36° cut LiTaO ₃	PVDF
Density (g/cm ³)	5.61	3.3	7.8	2.64	4.64	7.45	1.79
Moulus (GPa)	110–140	300–350	61	71.7		225	0.16
Hardness	4–5 GPa	15 GPa	7–18 GPa	Moh's 7	Moh's 5 Knoop 800–1000	70–110 Knoop 700–1200	Shore D75–85
Refractive index	1.9–2.0	1.96	2.40	1.46	2.29	2.18	1.42
Piezo-constant d ₃₃ (pC/N)	12	4.5, 6.4	289–380, 117	2.3 (d ₁₁)	19–27	–21	–35
Coupling coefficient, <i>k</i>	0.15–0.28, 0.33	0.17–0.5	0.49	0.0014	0.23	0.2	0.12–0.2
Effective coupling coeff. <i>k</i> ² (%)	1.5–1.7	3.1–8	20–35	8.8–16	2–11.3	0.66–0.77	2.9
Acoustic velocity by transverse (m/s)	6336 (2650)	11,050 (6,090)	4500 (2200)	5960 (3310)	3970	3230–3295	2600
Dielectric constant	8.66	8.5–10	380	4.3	85 (29)	54 (43)	6–8
Coefficient of thermal expansion (CTE, ×10 ^{–6})	4	5.2	1.75	5.5	15	–16.5	42–75

waves have a longitudinal component that can be coupled with a medium in contact with the device's surface. This coupling can transport the media on the surface during its propagation [31]. When liquid (either in bulk or droplet form) exists on the surface of a SAW device, the energy and momentum of the acoustic wave are coupled into the fluid at a Rayleigh angle, following Snell's law of diffraction (see Fig. 1) [32,33]. The Rayleigh angle, θ , is defined by

$$\theta = \sin^{-1} \left(\frac{v_l}{v_s} \right) \quad (2)$$

where v_l and v_s are the velocity of the longitudinal wave in solid and liquid. The energy and the momentum of the longitudinal wave radiated into the liquid can be harnessed for liquid pumping and mixing. A net pressure gradient, P , forms in the direction of the acoustic wave propagation and provides an effective force to drive the liquid, which can be described by [34]

$$P = \rho_0 v_s^2 \left(\frac{\Delta \rho}{\rho_0} \right)^2 \quad (3)$$

in which, ρ_0 is the liquid density and $\Delta \rho$ is the slight density change due to the acoustic pressure. The generated acoustic pressure can create significant acoustic streaming in a liquid and result in liquid mixing, pumping, ejection and atomization [35]. This allows rapid movement of liquid and also internal agitation, which speeds up biochemical reactions, minimizes non-specific biobinding, and accelerates hybridization reactions in protein and DNA analysis which is commonly used in proteomics and genomics [36,37]. Surface acoustic wave based liquid pumps and mixers [38,39], droplet positioning and manipulation [40], droplet ejection and atomization systems [41,42], and fluidic dispenser arrays [43] have been proposed and developed. They have distinct advantages, such as simple device structure, no moving-parts, electronic control, high speed, programmability, manufacturability, remote control, compactness and high frequency response [44–46].

2.3. Selection of bulk materials or thin films

Acoustic wave devices can be used for both bio-sensing and microfluidics applications, which are two of the major components for lab-on-a-chip systems. Therefore, it is attractive to develop lab-on-chip bio-detection platforms using acoustic wave devices as this integrates the functions of micro-droplet transportation, mixing and bio-detection. To date, most of the acoustic devices have been made from bulk piezoelectric materials, such as quartz (SiO₂), lithium tantalate (LiTaO₃), lithium niobate (LiNbO₃) and sapphire (Al₂O₃). These bulk materials are expensive, and are less easily integrated with electronics for control and signal processing. Piezoelectric thin films such as ZnO have good piezoelectric properties,

high electro-mechanical coupling coefficient, high sensitivity and reliability [47]. They can be grown in thin film form on a variety of substrates, including silicon, making them perhaps the most promising material for integration with electronic circuitry, aiming for disposal, low-price and mass production [48]. This approach is likely to be the future of acoustic wave based lab-on-a-chip bio-sensing devices.

ZnO, AlN and PZT are the three dominant piezoelectric thin film materials which can be integrated into MEMS and microelectronics processes. Gallium arsenide (GaAs), silicon carbide (SiC), polyvinylidene fluoride (PVDF) and its copolymers are less common thin film piezoelectric (PE) materials (see Table 2). Among these, PZT has the highest piezoelectric constant and electro-mechanical coupling coefficient. However, for biosensor applications, PZT films have disadvantages such as higher acoustic wave attenuation, lower sound wave velocities, and poor biocompatibility. Piezoelectric AlN thin films have a much higher phase velocity, and are hard and chemically stable (see Table 2). However, the deposition of AlN films and texture control are more difficult compared with that for ZnO. Other PE films are either too expensive such as GaAs and SiC or too weak in their piezoelectric effect, e.g., PE-polymers [49,50]. Compared with AlN, ZnO shows a higher piezoelectric coupling, and it is much easier to control the film stoichiometry, texture and other properties [51]. Zinc oxide is biosafe and therefore suitable for biomedical applications to immobilize and modify biomolecules without toxic effects [52]. This paper summarizes recent developments in the preparation and application of ZnO films for acoustic wave-based microfluidics and biosensors, and also discusses future trends for ZnO film based lab-on-a-chip applications.

3. Requirement for ZnO film for sensing and microfluidic applications

For the successful application of ZnO films for acoustic wave bio-sensing and microfluidic applications, there are some basic requirements which include:

- (1) Microstructure issues:
 - Strong texture.
 - High crystal quality and low defects.
 - Uniformity in film microstructure and thickness.
 - Smooth surface and low roughness.
 - Good stoichiometry (Zn/O ratio).
- (2) Good piezoelectric properties:
 - High frequency and large acoustic velocity.
 - High electro-mechanical coupling coefficient k^2 .
 - Low acoustic loss.
 - High quality factor Q .

- Good thermal or temperature stability (low thermal coefficient of frequency or velocity).
- (3) Fabrication requirement:
- Compatible with MEMS or CMOS technology.
 - Easy deposition on different substrates and complex shape.
 - High deposition rate.
 - Low cost and mass production.
 - Reproducibility/high yield.
 - Low film stress/good adhesion to substrates.
- (4) Microfluidics and biosensor:
- High sensitivity and selectivity.
 - Stability of performance.
 - High pumping/mixing efficiency.
 - Easy functionalization of surfaces for immobilization of antibodies.
 - Biocompatibility.

The following sections focus on recent progress covering the above issues.

4. ZnO film and piezoelectric properties

4.1. Deposition and microstructure

Many different methods have been reported for the deposition of ZnO films, including sol–gel processes, chemical vapour deposition, metal-organic chemical vapour deposition, sputtering, molecular beam epitaxy, pulsed laser deposition, filtered vacuum arc deposition and atomic layer deposition [53–56]. Table 3 compares different deposition methods for the ZnO films. From a MEMS fabrication point of view, radio-frequency (RF) magnetron reactive sputtering is one of the best methods, with good reproducibility and compatibility with planar device fabrication technology [57]. In this section, we will focus on the texture and acoustic wave properties of sputtered ZnO films.

The microstructure, texture and piezoelectric properties of the ZnO films are normally affected by sputtering conditions such as plasma power, gas pressure, and substrate material and temperature as well as film thickness. During sputtering, the energetic ion bombardment has significant effects on the stoichiometry, size, shape and orientation of ZnO crystals, intrinsic stress, defects, electrical and optical properties, as well as surface and cross-section morphologies. The effects of the processing parameters, such as sputtering gas pressure, RF power, total flux density, bias voltage and substrate temperature, have been successfully described using modified Thornton models [58,59]. Some general conclusions about the effects of sputtering parameters on ZnO thin films are summarized as follows:

- (1) Higher plasma or bias power results in a higher deposition rate because the deposited particles have higher kinetic energies. However, the film surface roughness could increase significantly at a higher power, due to the ion bombardment effect.

Table 3

A comparison of different types of deposition methods.

	Sputtering	CVD and MOCVD	Laser ablation	MBE	Sol–gel	FCVA
Epitaxial growth	Possible	Yes	Yes	Highly	Difficult	Possible
Deposition rate	Medium (a few nm/s)	Low (0.2 to a few nm/s)	Low (0.1 to 0.4 nm/s)	Very low	High	High (0.2–15 nm/s)
Compatibility with MEMS processing	Good	Ok	Poor	Poor	Good	Poor
Temperature	25–400 °C	300–900 °C	200–600 °C	300–800 °C	Room temperature	Low
Quality	Good	Good	Good	Excellent	Poor	Good
Cost	Slightly costly	Medium	Medium	High	Cheap	Medium
Deposition size	Large area	Large area	Small size	Medium	Large area	Small size

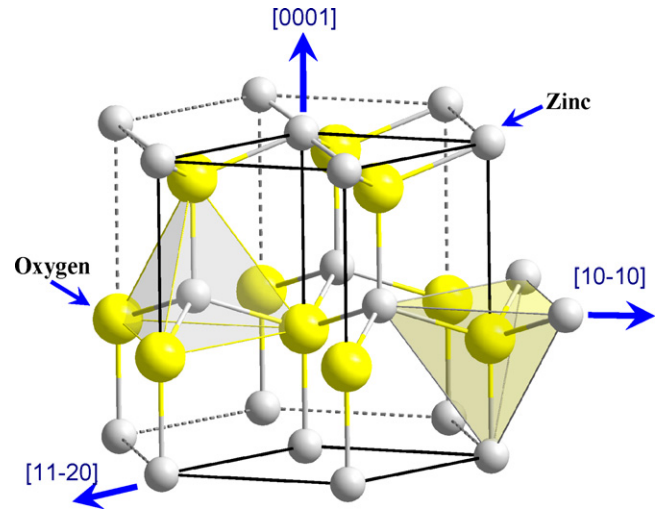


Fig. 2. ZnO crystalline structure–Wurtzite structure (modified following Ref. [1]) with directions of [0001], [11–20] and [10–10] indicated. The lattice constants are $a = 3.25 \text{ \AA}$ and $c = 5.2 \text{ \AA}$.

- (2) Low gas pressure generally results in a dense and fine grain film. Higher gas pressure could result in porous, columnar films with rough surfaces [60].
- (3) The gas ratio of O_2/Ar is a critical parameter and a sufficient oxygen partial pressure is needed to maintain the stoichiometry of the ZnO films.
- (4) ZnO thin films can be deposited at low temperature ($<200 \text{ }^\circ\text{C}$), which is compatible with existing CMOS circuitry on a chip. However, high temperature deposition will enhance the atom mobility, decrease the defects, promote film adhesion to the substrate, improve film texture, quality and increase grain size, resulting in a compact and dense film structure.
- (5) The sputtered film normally shows a good piezoelectric effect. Thus post-deposition poling to obtain a good piezoelectric effect is unnecessary.

4.2. Film texture

The film texture of the ZnO film is crucial for the piezoelectric and acoustic wave properties of the acoustic devices. The substrate has significant influences on nucleation, growth and texture, acoustic wave velocity/frequency, and electro-mechanical coupling coefficient of the ZnO acoustic wave devices.

4.2.1. Self-texture and wave mode

ZnO normally crystallizes in a hexagonal, quartzite type crystalline structure [61] (see Fig. 2), which is dominated by three crystal planes: (0001), (1010) and (1120), with their surface energy densities of 0.99, 0.123, and 0.209 eV/Å², respectively [62]. The (0001) plane has the lowest surface free energy. Therefore, under equilibrium, if there is no epitaxy between the film

Table 4
Summary of velocity of the ZnO films: (1) most data from SAW devices, (2) the data is only for comparison, as the velocity is related to the film thickness, thus the comparison of velocities is no meaning unless the film thickness is the same.

Device type	Substrate materials	Structure	Lattice difference	Velocity (m/s)	Temperature expansion coefficient (10^{-6} K^{-1})
ZnO	ZnO	HCP		2724	2.9 (4.751)
ZnO/Si	Si (1 1 1)	Cubic	41.3%	2653	3
ZnO/Pt	Pt (1 1 1)	Cubic	1.8%	2684	8.8
ZnO/Au	Au (1 1 1)	Cubic	2.5%		14
ZnO/SiO ₂	Quartz			4200	13.2 (a)/7.1c
Sapphire	Al ₂ O ₃ (0001)	HCP	31.8%	4000–5750	7.3 (18.1)
ZnO/LiNbO ₃	LiNbO ₃ (0001)	HCP			14.8 (4.1)
ZnO/sapphire	Sapphire (0001)	HCP	31.8%		8.4 (5.3)
ZnO/GaN	GaN	HCP	1.8%		3.17
ZnO/AlN	AlN	HCP	4.1%	4522	5.3 (4.1)
ZnO/DLC	DLC	Amorphous		5000–7000	
Nanocrystalline diamond				8500	1.18
ZnO/diamond	Diamond (1 1 1)	Cubic		10,000–12,000	1.18
ZnO/AlN/diamond	ZnO/AlN/diamond			12,200	

and substrate, or without any external energy source, the films exhibit self-texture and grow along the (0001) orientation, on both crystalline and amorphous substrates [63]. However, as the film thickness increases, the other orientation peaks might appear and become stronger [64]. Excess Zn during film growth can cause the deterioration of the ZnO film crystallinity [65]. The O₂/Ar gas ratio and gas pressure have frequently been reported to have significant effects on the film stress and texture [61–65].

ZnO acoustic wave devices with a (0001) film texture can be used for sensing in air or gaseous environments. However, many biosensors need to detect chemical reactions in a liquid environ-

ment. For bio-sensing in liquids, it is necessary to generate a shear horizontal mode wave, where the wave displacement is within the plane of the crystal surface [66,67]. For generation of such a shear horizontal wave, other film textures such as the (11 $\bar{2}$ 0) and (10 $\bar{1}$ 010–10) are necessary [68].

4.2.2. Interlayer or buffer layer

An amorphous ZnO intermediate layer is normally formed before the growth of the crystalline ZnO layer on substrates such as Ni, Cu, Si, Ti and glass, and this layer is about 10–50 nm depending on the type of substrates [69,70]. Self-textured (0001) ZnO films slowly grow on this amorphous layer, which is probably the reason why the ZnO films deposited on Ni, Cu, and Cr substrates show poor texture. No such amorphous interlayer was observed on Au, Ru, Pt, Al and sapphire substrates [71,72], and the ZnO films deposited on these substrates show good (0001) orientation. Buffer layers are frequently used to enhance the film crystalline quality and texture, for example, AlN, MgO, Al₂O₃, GaN, DLC, and SiO₂ (see Table 4) [73–75] and they can also be used to promote the epitaxial growth of ZnO films.

4.2.3. Epitaxial growth

Epitaxial growth on different substrates can lead to different ZnO orientations. The growth of ZnO can be attributed to the competition between the lowest surface free energy (0001) of ZnO and the closest lattice mismatch between the ZnO growth plane and the substrate plane (see Table 4) [76]. However, this is significantly dependent on the deposition methods and substrate materials. MBE, pulsed laser deposition, MOCVD and sputtering have been frequently been used to grow the ZnO epitaxial films [77,78]. The common substrates for epitaxial growth of the ZnO film include: quartz, sapphire, LiNbO₃, SrTiO₃, diamond, and MgO.

4.2.4. Oxygen ion bombardment

During ZnO sputtering, a directional oxygen ion beam, at an angle towards the substrate surface, plays an important role in changing the ZnO film texture from a (0001) texture into (10 $\bar{1}$ 0) or (11 $\bar{2}$ 0) texture due to ion channeling effect [79]. The ZnO films with these two textures can excite a shear acoustic wave without a longitudinal wave [80]. A pre-requisite for the significant oxygen ion bombardment effect is a low gas pressure which contributes to a longer mean free path for the oxygen ion bombarding the film surface. ZnO films at different positions on the substrate under plasma also show different crystal orientations (see Fig. 3) [81], which can easily be explained by the oxygen ion bombardment angle effects under the target.

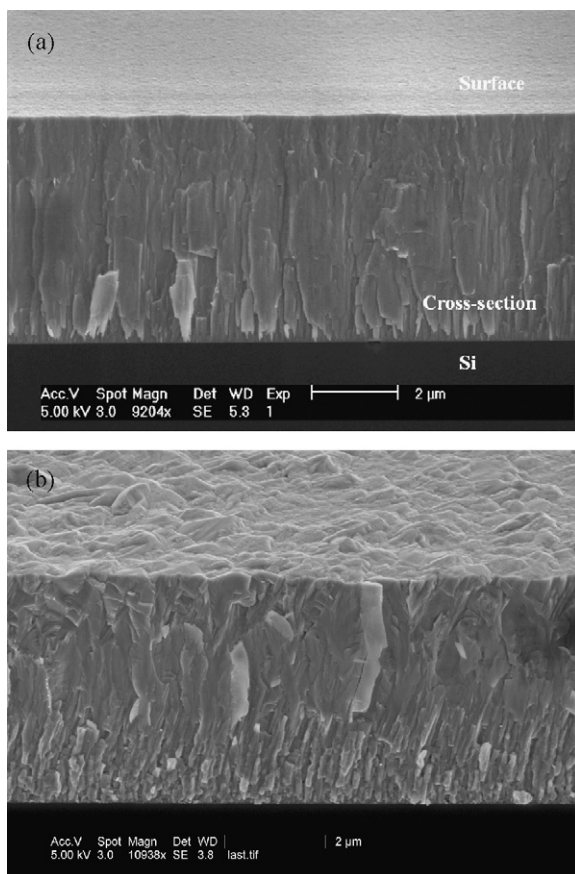


Fig. 3. SEM cross-section morphologies of ZnO films deposited using magnetron sputtering method: (a) under target; (b) far away from target showing the inclined structure due to ion channeling effect.

In summary, a (0001) film texture is commonly observed for the sputtered ZnO films. In order to obtain the other types of film texture, the following methods could be used:

- (1) Epitaxial growth on a specific substrate using a suitable deposition method;
- (2) controlling the sample position under the plasma [82];
- (3) using an additional anode near the substrate, which can have an apparent orientating effect on the growing films [83];
- (4) substrate tilting with a set angle due to the oblique incidence of the particles on the growing film;
- (5) using an external oxygen ion source and control the oxygen ion bombardment during film growth;
- (6) using a blind which can be positioned between the target and substrate to only allow oblique particles to be incident on substrate surface [84].

4.3. Piezoelectric properties of sputtered ZnO films

4.3.1. Substrate effect

The acoustic velocity of a ZnO film significantly depends on the substrate on which it is grown. The ZnO film deposited on a substrate with large acoustic velocity will exhibit an increased velocity value. Therefore, by selecting a substrate with a large acoustic velocity, the wave velocity in the ZnO SAW devices can be increased accordingly. For example, the acoustic velocity of bulk ZnO is 2724 m/s; it becomes 4522 m/s for ZnO/AlN; and up to 12,200 m/s for a ZnO/AlN/diamond substrate [85,86]. Table 4 summarizes the acoustic velocities of the ZnO films on different substrates. Among them, AlN, DLC, nano-diamond films and diamond are regarded as the best substrate materials to provide a dramatic increase in acoustic wave velocities in the ZnO films [87–89].

4.3.2. Film thickness effect

Acoustic velocity depends significantly on the ZnO film thickness for both the ZnO based SAW and FBAR devices.

4.3.2.1. *ZnO SAW devices.* The ZnO film thickness effect for a ZnO/Si SAW devices can be summarized as follows [90,91]:

- (1) For a SAW device made on a very thin ZnO thin film (less than hundreds of nanometers), the acoustic wave can penetrate much deeper into the substrate as the film thickness is normally much less than one wavelength. In this case, the energy of a SAW device is largely dissipated in the substrate, and the wave predominantly propagates in the substrate, thus the wave velocity of the SAW approaches the Rayleigh velocity of the substrate material as shown in Fig. 4a.
- (2) When the ZnO film thickness increases, the acoustic velocity gradually changes to that of ZnO film (about 2724 m/s). Therefore, by varying the thickness of the ZnO film, the phase velocity of the acoustic wave can vary between the acoustic velocities of the surface piezoelectric layer and the substrate material. However, there is normally a cut-off thickness, below which no wave mode can be detected, due to the low electro-mechanical coupling coefficient for a very thin ZnO film.
- (3) A Rayleigh-type wave (called the fundamental mode) can be generated when the film is thin. With increasing film thickness, a higher order acoustic wave mode known as the Sezawa wave can be obtained. A Sezawa mode is realized from a layered structure in which the substrate has a higher acoustic velocity than that of the overlying film [92]. This wave exhibits a larger phase velocity (higher resonant frequency) than that of the Rayleigh wave for a fixed thickness (see Fig. 3a), and is thus desirable for high frequency applications [93,94]. In a similar manner to

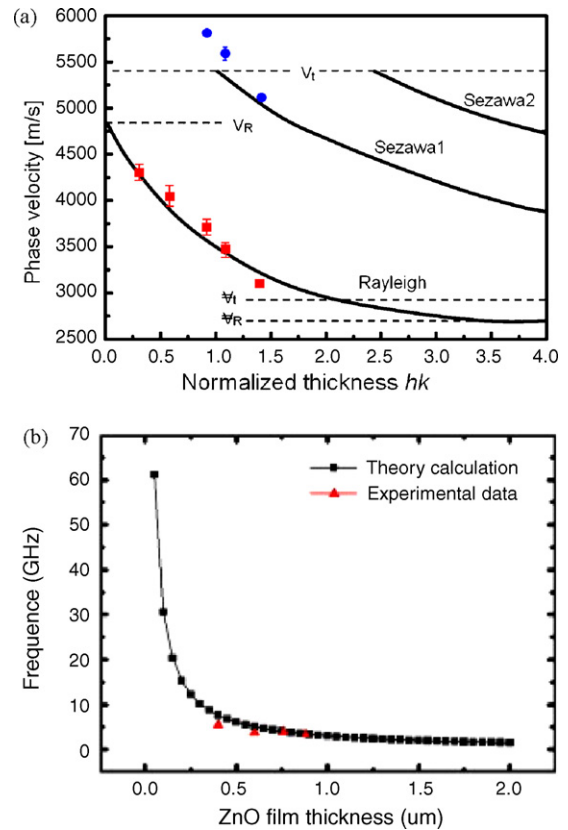


Fig. 4. (a) Phase velocities for the Rayleigh and Sezawa modes on different thickness of ZnO film. A film normalized thickness, hk , is used to describe the film thickness effect ($k = 2\pi/\lambda$: wave vector, h : film thickness) [90]; (b) resonant frequency of ZnO FBAR devices vs. film thickness [130].

that of Rayleigh wave, the resonant frequency and the phase velocity of the Sezawa wave decreases with film thickness.

- (4) For the ZnO/Si SAW devices, the metallization ratio (ratio of thickness of metal and ZnO film) of the IDTs affects the generation of the guided wave mode and its harmonics. For example, if the metallization ratio changes from 0.5 to 0.4 (or to 0.7) in the ZnO/Si devices, many higher-order odd harmonic waves, such as the Rayleigh mode 3rd or 5th harmonic, or 3rd Sezawa mode harmonic can be realized together with the fundamental one [95,96]. These higher mode harmonic waves can reach frequencies of a few GHz using conventional photolithography, which could avoid the necessity of using high acoustic velocity substrate materials (such as diamond) or an advanced lithography processes (such as e-beam or deep-UV lithography) to make IDTs with sub-micron arm widths.

4.3.2.2. *ZnO FBAR device.* For ZnO FBAR devices, the resonant frequency depends on: (a) the thickness and material type of the electrode layer; (2) the thickness ratio of the piezoelectric and electrode layers; (3) the material and thickness of the interlayer or buffer layer [97]. With the decrease in ZnO film thickness the frequency generally increases significantly, with one example shown in Fig. 4b [98,99]. However, there is a practical minimum thickness limitation for the ZnO film. If thin film is too thin, the frequency changes dramatically, but the peak intensity will decrease significantly with decrease in thickness (which becomes difficult to monitor).

4.3.3. Others

For ZnO acoustic wave devices, the most frequently used electrode material is aluminum. However, the lifetime of the Al

electrode in aqueous media is limited due to significant corrosion effects. The other common electrode materials include Au, Ni, W, Pt, Ta and Cu. The electro-mechanical coupling coefficient (k^2) of the ZnO/Si acoustic wave devices depends on [100,101]: (1) wave propagation mode (fundamentals or their harmonics); (2) normalized thickness of ZnO film; (3) film texture; (4) film thickness; (5) the nature and dimension of the electrodes; (6) substrate materials. The temperature coefficient of frequency (TCF) is an important parameter for ZnO FBAR and SAW applications for biosensors. There are different strategies to minimize the TCF or compensate for the temperature effect associated with ZnO based devices. The common strategy is to combine a material with a positive (or negative) TCF values, with another one with a negative (or positive) TCF. ZnO film has a negative TCF value, thus an easy way to reduce the TCF is to use a substrate or interlayer with a positive TCF value, such as SiO₂ or quartz [102].

5. MEMS processing of ZnO films

ZnO films normally have excellent bonding to a range of substrate materials. However, caution is required for MEMS processing of ZnO films as they are quite reactive and sensitive to temperature, acids as well as water [103]. In fact ZnO will dissolve in deionized water with a solubility of about 2 mg/l [104]. Hence, any rinsing of ZnO films using DI water should be made in as short a time as possible. Acetone can be used for cleaning the samples, but Pirana, or other strong cleaning solution should be avoided. In addition ZnO is easily hydrolyzed upon exposure to air. For MEMS processing, it is necessary to pre-bake the film and remove the moisture, thus improving the adhesion of photoresist. However, high temperature post-baking or annealing above 400 °C should be avoided.

Photoresist adheres well to clean and dry ZnO films. The improvement of photoresist adhesion can be improved by (1) pre-baking; (2) coating with other materials, such as SiO₂; (3) using an adhesion promoter. ZnO is soluble in most acids. Although different types of etchants, such as HCl, H₃PO₄, HF, HNO₃, alkalis, ammonium chloride and NH₄Cl + NH₄OH + H₂O can be used for removing ZnO, the etch profile is typically difficult to control. The recommended ZnO film etching solutions include [105]: (1) H₃PO₄ + HAc + H₂O (1:1:50); (2) FeCl₃ + 6H₂O.

ZnO can be etched using most plasma gases, including oxygen plasma. For dry etching of ZnO films with a photoresist mask, there are two types of gas systems which have been frequently used [106]: (a) hydrogen based gases such as CH₄/H₂/Ar which can help in obtaining an anisotropic etch profile; (b) chlorine based gases, such as Cl₂/Ar, BCl₃/Ar and BCl₃/Cl₂/Ar plasma which are toxic. Recently, a new plasma etching method using a remote Ar/H₂ plasma has been developed, in which the hydrogen ions contribute to efficient and fast etching [107]. Inductively coupled plasma reactive ion etching has also used to anisotropically etch ZnO films using HBr/Ar plasma with photoresist as the etch mask [108]. The etching of ZnO films in the HBr/Ar gas mixture is controlled by chemically assisted sputter etching.

As regards microfluidic applications, ZnO is hydrophilic with a contact angle typically of 50–80°, which is dependent on surface conditions and light exposure [109]. Ultraviolet irradiation of ZnO film results in a superhydrophilic surface [110]. For efficient droplet pumping, a hydrophobic surface is normally needed and methods for improving the hydrophobic properties of the ZnO films include [111–113]: (1) spin coating PTFE (Teflon); (2) a monolayer of octadecyl thiol (ODT); (3) a monolayer of octadecylsilane (ODS); (4) an octadecyltrichlorosilane (OTS) self-assembled monolayer (SAM). After such treatment, the contact angle can be as high as 100–120°.

A critical issue in developing a high performance biosensor is to find a simple and reliable process for functionaliza-

tion of the ZnO surface through a covalent method to form a robust immobilization of appropriate probe molecules. Normally Au is pre-deposited on the ZnO surface, and a cystamine surface atomic monolayer (SAM) is formed on the Au surface to which antibodies will attach. Currently little work has been performed on the direct surface functionalization of the ZnO films. Initial studies for immobilization of antibodies on the ZnO film surface have been realized using [114,115] (1) amine-terminated silane, 3-aminopropyltriethoxysilane, and glutaraldehyde as the secondary crosslinker to bind a protein; (2) 3-mercaptopropyltrimethoxysilane in dry toluene; or (3) trimethoxysilane in dry toluene to immobilize the antibody. As Au is not recognised as a good CMOS compatible material, the direct immobilization on the ZnO film has its advantages for bio-sensing applications.

6. ZnO acoustic devices for biosensor and microfluidics

6.1. Biosensor applications

6.1.1. ZnO SAW biosensor

A ZnO/Si SAW device has been successfully used in the detection of PSA antibody-antigen immuno-reaction as a function of PSA concentrations [116]. The resonance frequencies of the ZnO SAW devices were found to shift to lower frequencies as the PSAs are specifically immobilized on the surface-modified ZnO SAW device. A linear dependence was found between the resonance frequency change and the PSA/ACT complex concentrations over the broad dynamic range of 2–10,000 ng/ml [140]. However, as discussed before, a big challenge for SAW biosensors is how to realize detection in a liquid environment. SH or Love mode SAW devices are promising technologies for biosensors used in liquid environments because of their high sensitivity and low energy dissipation. The essential condition for a Love-wave mode is that the shear wave velocity in the surface wave guide layer is smaller than that in the piezoelectric substrate. For example, ZnO has a shear wave velocity of 2578 m/s, whereas those of ST-cut-quartz and SiO₂ are 4996 and 3765 m/s, respectively. Therefore, it is reasonable to use ZnO as a guiding layer on substrates of ST-cut quartz to form Love mode biosensors. The other potential substrate materials for Love-mode ZnO sensors include LiTaO₃, LiNbO₃ and sapphire. A ZnO Love mode device of ZnO/90° rotated ST-cut quartz has a maximum sensitivity up to $-18.77 \times 10^{-8} \text{ m}^2 \text{ s kg}^{-1}$, which is much higher than that of a SiO₂/quartz Love mode SAW device [117–119].

Most of the above mentioned ZnO Love mode sensors are based on a bulk piezoelectric substrate (for example, quartz, LiNbO₃ and LiTaO₃), which are expensive and incompatible with IC fabrication. In reference [120], ZnO/SiO₂/Si SAW Love mode sensors were studied, and the sensitivity of the devices as high as 8.64 μm²/mg (with an acoustic wave velocity of 4814.4 m/s) were reported, which is about 2–5 times that of ZnO/LiTaO₃ [121] and SiO₂/quartz Love sensors [122]. Another promising approach for making a ZnO based Love mode sensor is to use a polymer film (such as PMMA, polyimide, SU-8 or parylene C) on top of the ZnO layer as the guiding layer. This polymer waveguide layer structure however, has a relatively larger intrinsic attenuation than those of solid waveguide layers.

6.1.2. ZnO Lamb biosensor

In Lamb wave sensors, the wave propagation velocity in the membrane is slower than the acoustic wave velocity in the fluids on the surface, thus the energy is not easily dissipated and can be used in liquid samples [123]. A ZnO based Lamb wave device has been used to monitor the growth of bacterium "Pseudomonas putida" in a boullus of toluene, as well as the reaction of antibodies in an immunoassay for an antigen present in breast cancer patients

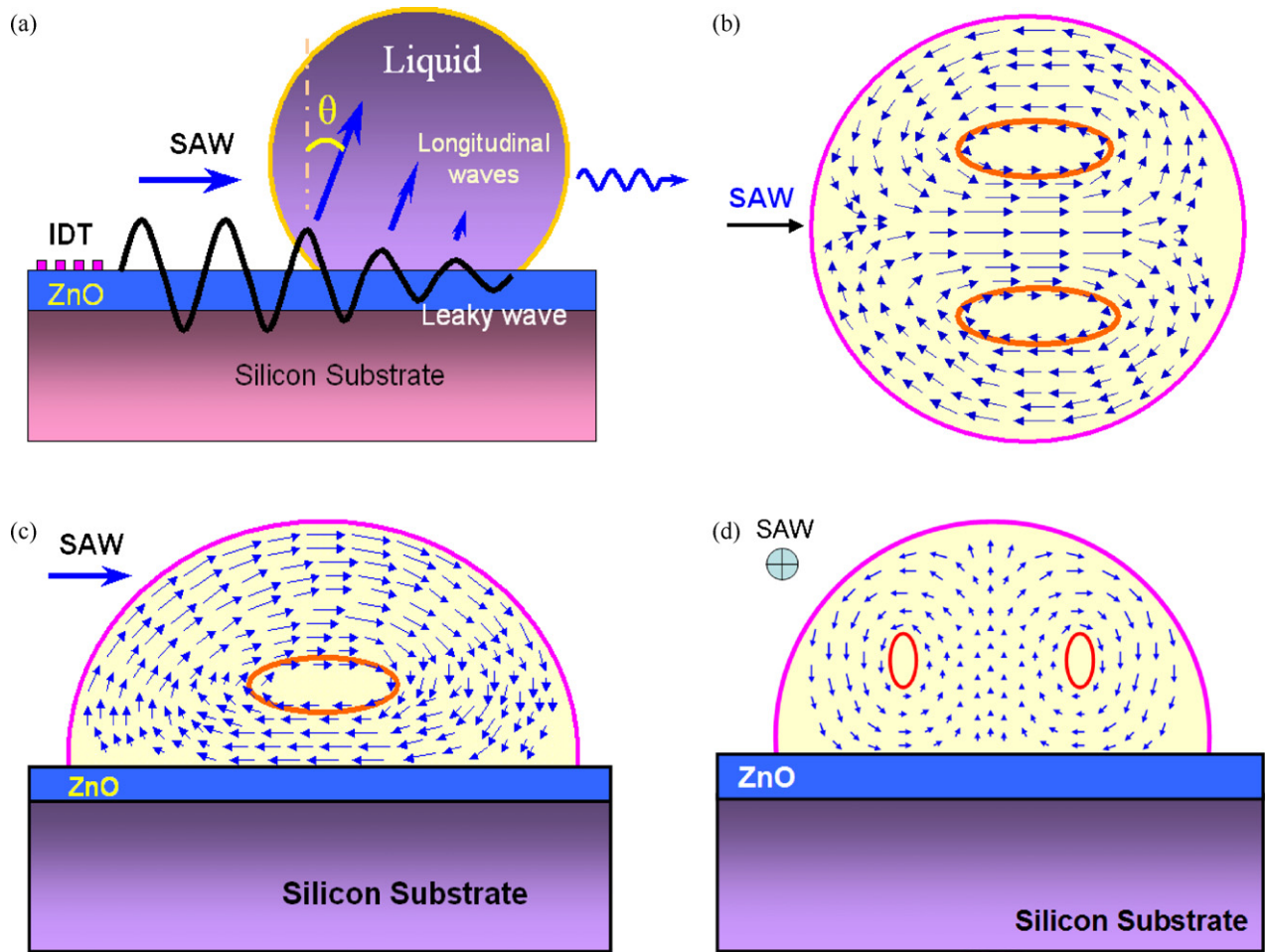


Fig. 5. (a) Interaction between SAW and a liquid droplet on a ZnO based SAW devices; (b) top view; (c) cross-section view; (d) front view of the internal streaming inside the droplet on the ZnO surface.

[124]. A Si/SiO₂/Si₃N₄/Cr/Au/ZnO Lamb wave device has been used for detecting human IgE based on conventional cystamine SAM technology, with a sensitivity as high as $8.52 \times 10^7 \text{ cm}^2/\text{g}$ at a wave frequency of 9 MHz [125]. In recent years, however, the Lamb wave biosensor has not been widely studied because of: (1) low sensitivity due to the low operation frequency; (2) difficulties in fabrication of thin and fragile membrane structures.

6.1.3. ZnO FBAR biosensor

FBAR biosensors have recently attracted great attention due to their inherent advantages compared with SAW and QCM biosensors: high sensitivity, low insertion loss, high power handling capability and small size [126,127]. High frequency ZnO FBAR sensors have good sensitivity and high energy densities owing to the trapping of the standing wave between the two electrodes, allow-

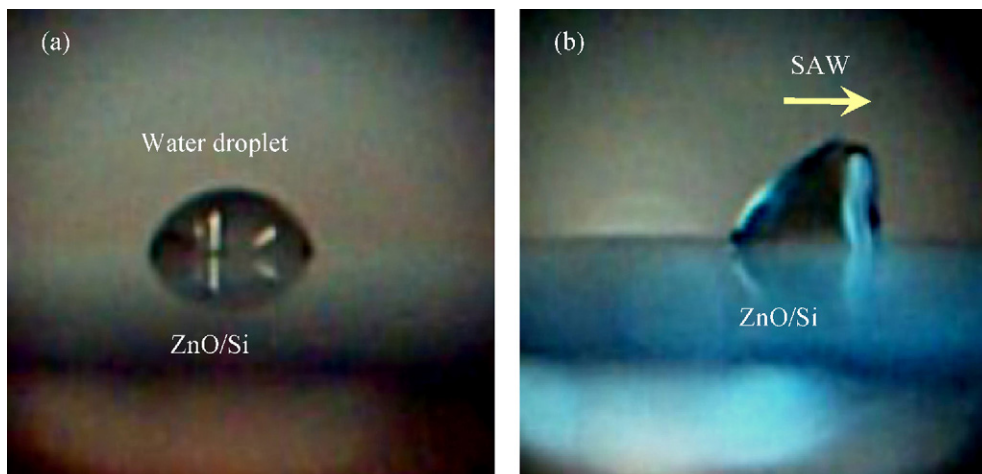


Fig. 6. A 2 µl water droplet in (a) and its movement along with the propagating acoustic wave in (b) showing the droplet is pushing upward and forward.

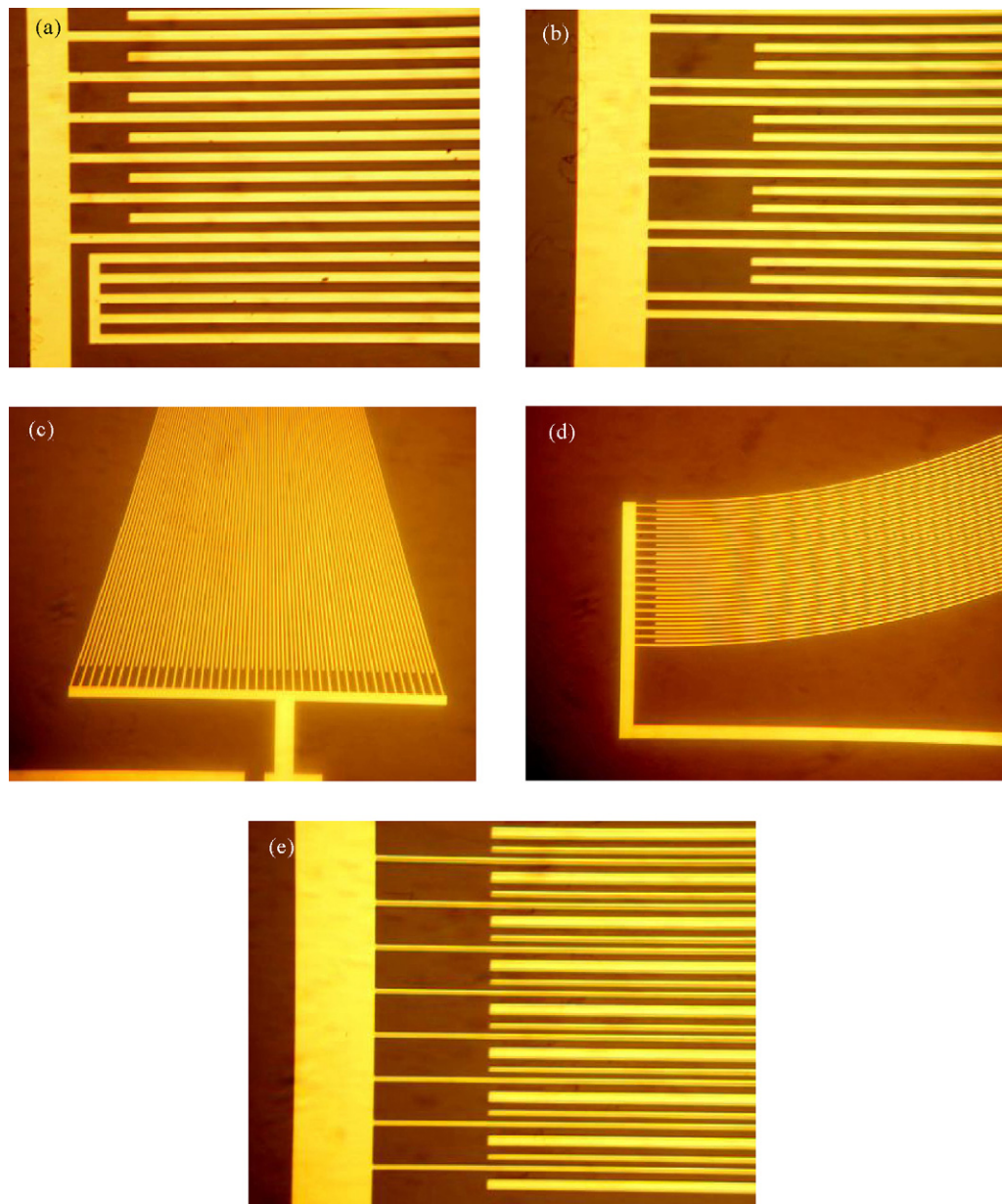


Fig. 7. SAW IDT designs. (a) SAW IDT with reflector; (b) splitted IDT; (c) angled IDT; (d) curved IDT; (e) SPUDT IDT design.

ing device size to be scaled down to areas more than three orders of magnitude smaller than the SAW and QCM devices. This makes the integration of FBAR arrays for parallel detection feasible and at low cost. In Ref. [128], a label free FBAR gravimetric biosensor based on a ZnO film was used to detect DNA and protein molecules with a high operating frequency of 2 GHz. Its sensitivity of $2400 \text{ Hz cm}^2/\text{ng}$ is about 2500 times higher than a conventional QCM device with a frequency of 20 MHz. A recent study using a Al/ZnO/Pt/Ti FBAR design showed a sensitivity of $3654 \text{ kHz cm}^2/\text{ng}$ with a good thermal stability [129,130].

Conventional ZnO (0001) textured FBARs operate using a longitudinal wave and cannot be used for sensing in a liquid environment. In contrast, a ZnO (11 $\bar{2}$ 0) textured hexagonal film exhibits pure shear modes waves which can propagate with little damping effect in a liquid. A ZnO shear mode FBAR device has been used in a water-glycerol solution, and showed a high operating frequency of 830 MHz and a sensitivity of $1000 \text{ Hz cm}^2/\text{ng}$ [131]. Weber et al. [132] have fabricated a ZnO FBAR device, which oper-

ates in a transversal shear mode, using a ZnO film with 16° off *c*-axis crystal orientation. The fabricated device has a high sensitivity of $585 \text{ Hz cm}^2/\text{ng}$ and mass detection limit of 2.3 ng/cm^2 for an avidin/anti-avidin biorecognition system. This shear wave FBAR device was also reported to have a stable temperature coefficient of frequency [133].

6.2. ZnO film for microfluidic applications

6.2.1. ZnO SAW mixer and pump

In a ZnO SAW device, the interaction between the longitudinal acoustic wave and liquid droplets can cause an acoustic streaming effect, and establish a stable streaming pattern with a double vortex (see Fig. 5a–d). The SAW streaming effect induces an efficient mixing and agitation within the droplets, which can be utilized to produce good micromixers [134]. With a large input RF voltage applied to the IDTs on a ZnO film, the water droplet becomes apparently deformed from its original shape (following the Rayleigh

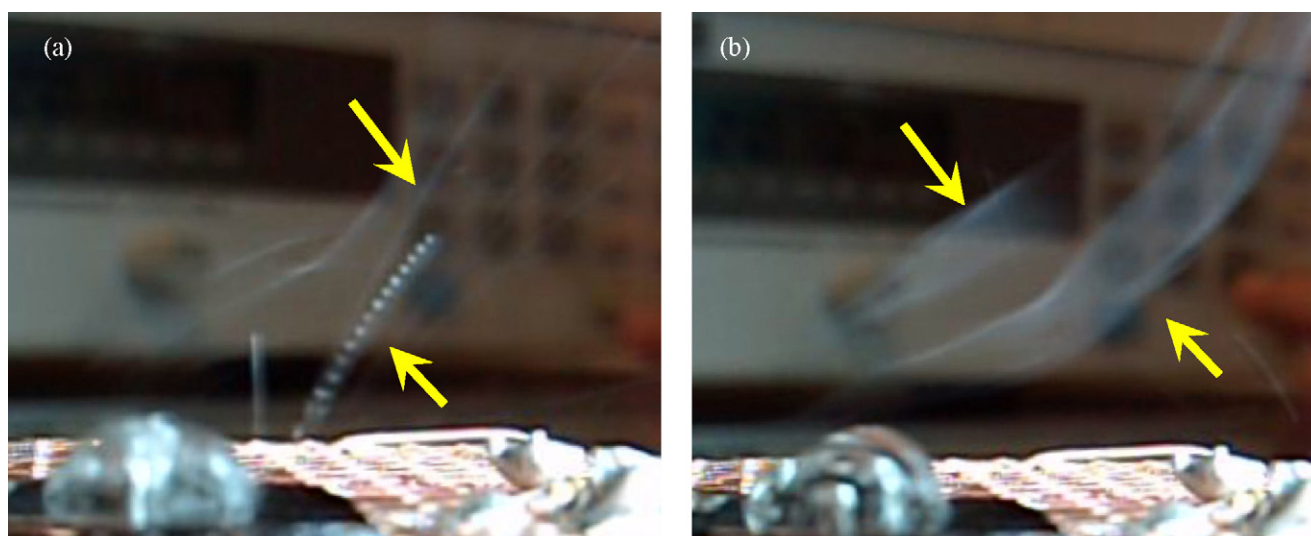


Fig. 8. Surface droplet ejection (a) and atomization process (b) on a ZnO SAW device.

angle) with an increased leading edge contact angle and decreased trailing edge contact angle. The large SAW pressure excites and stirs the droplet, causing it to vibrate along with the SAW. After surface hydrophobic treatment, the liquid droplets can be pumped forward with a voltage as low as ~ 20 V (see Fig. 6). The movement of the droplet is a combination of rolling and sliding, which is also dependent upon the power applied and the droplet size. The SAW IDT design is important for efficient SAW streaming/pumping. The conventional bidirectional IDT may not be efficient for pumping, as the wave propagates in two different directions with half of the energy wasted. The easiest way to solve this problem is to use reflectors to reflect back some of the wave (see Fig. 7a). More sophisticated IDT designs include [135,136]: (a) split IDTs (Fig. 7b); (b) a SPUDT (single phase unidirectional transducer, Fig. 7c) which shows internally tuned reflectors within the IDT to form a unidirectional SAW propagation from one side of the IDT; (c) focused or semi-circular IDT designs to focus the acoustic energy and increase the pumping efficiency; (d) a slanted IDT (see Fig. 7d), which has a broad range of resonant frequencies, and can be used to alter the directions of streaming and droplet movement [137].

As discussed before, ZnO is very reactive with acids, liquids, or moisture, and it will dissolve if exposed to water or a humid environment. To solve this problem, an “island” ZnO SAW structure is proposed in Ref [138] which can avoid direct contact between the ZnO active layer and the fluid being pumped. In this design, the ZnO film is only beneath the SAW IDTs. The acoustic waves generated on the ZnO film can continuously travel in the Si substrate without a ZnO film on top of the wave path. This offers great flexibility in the fabrication of highly integrated microfluidics with the SAW devices built on isolated ZnO islands while other components such as the microchannels, chamber and sensors being directly fabricated on the Si substrate.

6.2.2. ZnO SAW heating/droplet ejector

Higher RF power applied to a SAW device could generate fast streaming, hence a higher mixing and pumping efficiency. However, high RF power will also induce localized heating. The surface temperature of the ZnO SAW device increases with increase in voltage amplitude and duration of the RF signal, and decreases with the distance from the IDT. The maximum temperature reaches ~ 140 °C for the highest voltage amplitude of 60 V [90]. Significant acoustic heating is detrimental for the biosubstances being investigated, vapourising the liquid, and inducing severe detection errors due to temperature-induced resonant frequency shift. For ZnO SAW based

liquid transportation and mixing, heating effects can be suppressed by using a pulsed RF signal with temperature well controlled below 40 °C. A pulsed RF signal can also be used to control the droplet motion, as this offers more precise control of the distance moved and the droplet positioning [138]. Although acoustic heating has many negative effects for bio-sensing, controlled acoustic heating can be utilized as a remote heater for biomedical and life-science applications, such as in polymeric chain reactions (PCR) to amplify the DNA concentration for detection and in others to accelerate bio-reaction processes.

When the RF power applied to the IDT of a ZnO SAW device is sufficiently high, tiny liquid droplets will be ejected from the surface (see Fig. 8a). This has also been frequently reported for LiNbO₃ SAW devices [139]. Ejection of small particles and liquids has many applications ranging from inkjet printing, fuel and oil ejection and biotechnology. The authors have recently demonstrated that thin film ZnO based SAW devices can eject the droplets which are so tiny that an atomization process occurs as shown in Fig. 8b. In general, the ejected or atomized droplets from a SAW device have a large range of sizes and can only be ejected at a fixed Rayleigh angle.

6.2.3. ZnO SAW particle manipulation

Transportation and concentration of particles or biosubstances are one of the important issues for microfluidic and biosensor applications. A SAW can be utilized to concentrate and transport nano-/microparticles dispensed in liquid droplets. When a droplet is located on the SAW surface, an acoustic force will introduce a shear component and generate a single circular streaming pattern within the droplet. The shear velocity is high on the edge of the droplet, and gradually decreases on approaching the center of the droplet. The particles circulate with the liquid in the droplet and simultaneously migrate from high to low shear velocity regions [140]. The concentration effect is dependent on the RF power and amplitude of the SAW, as well as the properties of the particles [141]. At very low or very high powers, the particles become dispersed. The particle size is also critical and certain sizes will easily agglomerate, but particles that are smaller can flow inside the liquid. Therefore, it is possible to separate the particles according to their size using a SAW device [142].

6.2.4. ZnO membrane based microfluidics devices

Flexural plate waves or Lamb waves have also been proposed for pumping, agitating and enhancing biochemical reactions [143],

with the principle that fluid motion via the traveling flexural wave in a ZnO membrane can be used for the transport of liquids resulting in a steady flow of a few mm/s to cm/s in water [144]. The potential applications include a micro-total analysis system (μ TAS), cell manipulating systems, and drug delivery systems [145]. However, due to the low frequency resulting from the thin membrane, the agitation is not significant as there is insufficient energy coupled into the liquid.

A recent development using a ZnO membrane based acoustic wave device and self-focusing acoustic transducer successfully demonstrated that liquid can be pumped by strong acoustic streaming [146]. These membrane based acoustic wave devices have also been used to transport and trap particles, or to sort cells, with the principle that acoustic streaming produced at the interface of the membrane and fluid can actuate the particles in the liquid [147]. There are also some reports of new designs using ZnO acoustic wave devices as droplet ejectors [148]. Annular Fresnel ring (with different opening angles) half-wave band electrodes were used on the surface of a ZnO film as the self-focusing acoustic transducer, and a directional liquid droplet with different ejection angles can be generated by changing the opening angle of the sectored electrodes [149].

7. Future trends for ZnO devices and lab-on-a-chip

The elements required for operating a lab-on-a-chip for detection include: (1) transportation of liquids as blood or biofluid containing DNA/proteins into an area on which probe molecules have been pre-deposited, (2) mixing/reaction of the extracted DNA or proteins with oligonucleotide or the antibody binders, and (3) detection of an associated change in the physical, chemical, mechanical or electrical signals. As discussed in this paper, the acoustic wave generated on ZnO acoustic devices could induce significant acoustic streaming, and thus result in mixing, pumping, ejection and atomization of liquids (samples and reagents). ZnO acoustic wave devices can also be used as biosensors as discussed above. Therefore, ZnO based acoustic wave devices can be used to fabricate lab-on-chip bio-detection systems, which combine the functions of micro-droplet transportation, mixing and bio-detection [116].

ZnO based acoustic wave technologies can be integrated with other technologies, such as the surface plasma resonance (SPR) method [150]. SPR sensor technology has been commercialized and SPR biosensors have become a central tool for characterizing and qualifying biomolecular interactions. A combination of SAW-microfluidics and SPR sensing would appear to be sensible for both microfluidics and bio-detection functions. A potential problem is that the surface temperature change induced by acoustic excitation may cause changes in refractive index, which is used for SPR sensor detection. A pulse mode SAW signals can be used to minimize this effect. ZnO based acoustic wave microfluidic devices can also be combined with liquid chromatography or gas chromatography, which can be used to identify the protein or molecules by mass spectroscopy [151]. Integration of a SAW with optical methods enables the simultaneous qualification of biological soft layers formed on the sensor surface under different conditions, such as density, viscosity, thickness and water content.

For digital microfluidics, there is a need to precisely and continuously generate liquid droplets. ZnO acoustic wave technology can be used for the ejection of liquid droplets, but it is rather difficult to precisely control the micro-droplet generation. A potential technology to overcome the drawbacks is to combine electrowetting-on-dielectrics (EWOD) [152] with SAW-microfluidics. In the past 10 years, EWOD technology has been successfully developed to dispense and transport nanolitre to microlitre bio-samples in droplet form at the exact volume required

[153]. However, one of the weaknesses of the EWOD technology is that it does not provide efficient micro-mixing, and requires the integration of other technologies e.g. CMOS to realize bio-reaction and bio-sensing. A novel idea is to integrate the ZnO SAW/FBAR device with the EWOD device to form lab-on-a-chip equipped with well developed functionalities of droplet generation, transportation by EWOD, mixing and bio-sensing using a SAW/FBAR device [154].

Acoustic wave devices can be easily integrated with standard CMOS technology. Dual acoustic wave devices can be fabricated next to each other, so that the neighboring devices can be used as a sensor-reference combination. One of the devices without pre-deposited probe molecules can be used as a reference, while the other one with probe molecules can be used to sense. Using such a combination, the errors due to temperature drift or other interference on the sensing measurement can be minimized. Multi-sensor arrays can easily be prepared on a chip and a judicious selection of different immobilized bio-binders enables the simultaneous detection of multiple DNA or proteins, leading to an accurate diagnosis of a disease or detection of multiple diseases in parallel. The creation of these cost-effective sensor arrays can increase the functionality in real time and provide parallel reading functions.

Currently, one limitation of acoustic wave device applications is that they require expensive electronic detection systems, such as network analyzers. A final product aimed at the end user market must be small, portable and packaged into a highly integrated cost effective system. The detection of a resonant frequency can be easily realized using standard oscillator circuits which can measure the sensor losses based on a portable device. The required purposely built electronics for acoustic wave sensing is under development, but at present they are still bulk and heavy. Fabrication of portable ZnO based acoustic wave detection devices is also promising to enable the minimization of the system and the reduction of the power assumption. A wireless RF signals can be used to remotely measure or monitor physical, chemical and biological quantities by using acoustic wave devices, without the need of a power supply. Currently for a lab-on-chip device, sample pre-treatment, purification and concentration, as well as a good interface between the user and the integrated sensing system also need to be developed. A simple, robust, cheap packaging method is also critical for commercialization.

Currently, there is one concern that ZnO film is very reactive, and unstable even in air or moisture. Therefore, the stability and reliability becomes a big problem. To solve this problem, an "island" ZnO SAW structure mentioned in Section 6.2.1 can be used which can avoid direct contact between the ZnO active layer and the fluid being pumped. Deposition of a thin protection layer such as DLC and Si_3N_4 on top of the ZnO film will be another method. Compared to ZnO, AlN shows a slightly lower piezoelectric coupling. However, AlN films have some excellent properties. The Rayleigh wave phase velocity in (001) AlN is much higher than ZnO, which suggests that AlN is preferred for high frequency and high sensitivity applications [155]. AlN is a hard material with bulk hardness similar to quartz, and is chemically stable at temperatures less than about 700 °C. Therefore, using AlN could be an alternative and lead to the development of acoustic devices operating at higher frequencies, with improved sensitivity and performance in insertion loss and resistance in harsh environments [156].

8. Conclusions

ZnO films have good piezoelectric properties and a high electro-mechanical coupling coefficient, and are promising for the fabrication of fully automated and digitized microsystems with low cost, fast response, reduced reagent requirement and precision. In this paper, recent development on preparation and application of

ZnO films for acoustic wave-based microfluidics and biosensors has been discussed. High quality and strongly textured ZnO thin films can be prepared using RF magnetron sputtering. However, the microstructure, texture and piezoelectric properties of the ZnO films are affected by sputtering conditions such as plasma power, gas pressure, substrate material and temperature as well as film thickness. In addition the acoustic velocity of the ZnO film is dependent significantly on the substrate, film thickness and orientation.

ZnO acoustic wave devices can be successfully used as biosensors, based on a biomolecule recognition system. Among these biosensors, Love-wave devices, and surface acoustic wave and film bulk acoustic resonator devices using inclined ZnO films are promising for applications in highly sensitive bio-detection systems for both dry and liquid environments. The acoustic wave generated on the ZnO acoustic devices can also induce significant acoustic streaming, which can result in mixing, pumping, ejection and atomization of the fluid on the small scale depending on the wave mode, amplitude and surface condition. An integrated lab-on-a-chip diagnostic system based on these ZnO acoustic wave technologies is promising, and other functions such as droplet creation, cell sorting, as well as precise bi-detection can be obtained by integration with other advanced technologies.

Acknowledgements

The authors would like to acknowledge financial support from the Edinburgh Research Partnership in Engineering and Mathematics (ERPem). Y.Q. Fu would like to acknowledge support from the Royal Society of Edinburgh and Carnegie Trust. AJF, WIM and JKL would like to acknowledge the support of the EPSRC under grant no. EP/F063865/1 and EP/F06294X/1. AJW and YL acknowledge the support from The EU (GOLEM STRP 033211) and BBSRC.

References

- [1] D.S. Ballantine, R.M. White, S.J. Martin, A.J. Ricco, E.T. Zellers, G.C. Frye, H. Wohltjen, *Acoustic Wave Sensors, Theory, Design and Physical-Chemical Applications*, Academic Press, 1996.
- [2] M. Hoummady, A. Campitelli, W. Wlodarski, *Smart Mater. Struct.* 6 (1997) 647.
- [3] D.W. Galipeau, P.R. Sory, K.A. Vetelino, R.D. Mileham, *Smart Mater. Struct.* 6 (1997) 658.
- [4] P. Luginbuhl, S.D. Collins, G.-A. Racine, M.-A. Grétilat, et al., *J. Microelectromech. Syst.* 6 (1997) 337.
- [5] R. Lucklum, P. Hauptmann, *Meas. Sci. Technol.* 14 (2003) 1854.
- [6] W.J. Grate, S.J. Martin, R.M. White, *Anal. Chem.* 65 (21) (1993) 940A.
- [7] S. Shiokawa, J. Kondoh, *Jpn. J. Appl. Phys.* 43 (2004) 2799–2802.
- [8] H. Wohltjen, et al., *Acoustic Wave Sensor—Theory, Design, and Physico-Chemical Applications*, Academic Press, San Diego, 1997, p. 39.
- [9] G.L. Cote, R.M. Lec, M.V. Pishko, *IEEE Sens. J.* 3 (2003) 251–266.
- [10] L.A. Kuznestsova, W.T. Coakley, *Biosens. Bioelectron.* 22 (2007) 1567–1577.
- [11] F.R.R. Teles, L.P. Fonseca, *Talanta* 77 (2008) 606–623.
- [12] M.J. Vellekoop, *Ultrasonics* 36 (1998) 7.
- [13] S. Shiokawa, J. Kondoh, *Jpn. J. Appl. Phys.* 43 (2004) 2799.
- [14] E. Gizeli, *Smart Mater. Struct.* 6 (1997) 700.
- [15] K. Lange, B.E. Rapp, M. Rapp, *Anal. Bioanal. Chem.* 391 (2008) 1509–1519.
- [16] K.A. Marx, *Biomacromolecules* 4 (2003) 1099.
- [17] N. Barie, M. Rapp, *Biosens. Bioelectron.* 16 (2001) 978.
- [18] G. Kovacs, M. Venema, *Appl. Phys. Lett.* 61 (1992) 639.
- [19] F. Josse, F. Bender, R.W. Cernosek, *Anal. Chem.* 73 (2001) 5937.
- [20] G. Mchale, *Meas. Sci. Technol.* 14 (2003) 1847.
- [21] G. Lindner, *J. Phys. D* 41 (2008) 123002.
- [22] G. Kovacs, G.W. Lubic, M.J. Vellekoop, A. Venema, *Sens. Actuat. A* 43 (1992) 38–43.
- [23] B. Jacoby, M. Vellekoop, *Smart Mater. Struct.* 6 (1997) 668–679.
- [24] P. Murali, N. Ledermann, J. Baborowski, et al., *IEEE Trans. Ultrason. Ferroelectr. Freq. Control* 52 (2005) 2276.
- [25] N.T. Nguyen, R.M. White, *IEEE Trans. Ultrason. Ferroelectr. Freq. Control* 47 (2000) 1463.
- [26] Ph. Luginbuhl, S.D. Collins, G.-A. Racine, M.-A. Grétilat, N.F. de Rooij, K.G. Brooks, N. Setter, *Sens. Actuat. A* 64 (1998) 4119.
- [27] R. Ruby, *IEEE Ultrasonics Symp. Proc.* 1–6 (2007) 1029–1040.
- [28] D.A. Buttry, M.D. Ward, *Chem. Rev.* 92 (1992) 1355.
- [29] N.Y. Nguyen, Z.G. Wu, *J. Micromech. Microeng.* 15 (2005) 1.
- [30] J.K. Luo, Y.Q. Fu, Y.F. Li, X.Y. Du, A.J. Flewitt, A. Walton, W.I. Milne, *J. Micromech. Microeng.* 19 (2009) 054001.
- [31] M. Kuribayashi, M. Kurosawa, *Ultrasonics* 38 (2000) 15–19.
- [32] A. Wixforth, *Superlattices Microstruct.* 33 (2004) 389.
- [33] S. Shiokawa, Y. Matsui, T. Morizum, *Jpn. J. Appl. Phys.* 28 (1989) 126.
- [34] M. Rotter, A.V. Kalameitsev, A.O. Govorov, W. Ruile, A. Wixforth, *Phys. Rev. Lett.* 82 (1999) 2171.
- [35] M.I. Newton, M.K. Banerjee, T.K.H. Starke, S.M. Bowan, G. McHale, *Sens. Actuat.* 76 (1999) 89.
- [36] A. Toegl, R. Kirchner, C. Gauer, A. Wixforth, *J. Biomed. Technol.* 14 (2003) 197.
- [37] A. Wixforth, C. Strobl, C. Gauer, A. Toegl, J. Sciba, Z.V. Guttenberg, *Anal. Biomed. Chem.* 379 (2004) 982.
- [38] W.K. Tseng, J.L. Lin, W.C. Sung, S.H. Chen, G.B. Lee, *J. Micromech. Microeng.* 16 (2006) 539.
- [39] K. Sriharan, C.J. Strobl, M.F. Schneider, A. Wixforth, *Appl. Phys. Lett.* 88 (2006) 054102.
- [40] A. Sano, Y. Matsui, S. Shiokawa, *Jpn. J. Appl. Phys.* 37 (1998) 2979.
- [41] K. Chono, N. Shimizu, Y. Matsu, J. Kondoh, S. Shiokawa, *Jpn. J. Appl. Phys.* 43 (2004) 2987.
- [42] N. Murochi, M. Sugimoto, Y. Matui, J. Kondoh, *Jpn. J. Appl. Phys.* 46 (2007) 4754.
- [43] C.J. Strobl, Z. Guttenberg, A. Wixforth, *I.E.E.E. Trans. Ultrasonics, Ferroelectric Freq. Control* 51 (2004) 1432.
- [44] A. Renaudin, P. Tabourier, V. Zhang, J.C. Camart, C. Druon, *Sens. Actuat. B* 113 (2006) 387.
- [45] A. Toegl, J. Scribe, A. Wixforth, C. Strobl, C. Gauer, Z.V. Guttenberg, *Anal. Bioanal. Chem.* 379 (2004) 69.
- [46] T.A. Franke, A. Wixforth, *Chem. Phys. Chem.* 9 (2008) 2140–2156.
- [47] S.J. Pearton, D.P. Norton, K. Ip, Y.W. Heo, T. Steiner, *Prog. Mater. Sci.* 50 (2005) 293.
- [48] P. Murali, *J. Am. Ceram. Soc.* 91 (2008) 1385–1396.
- [49] S.Y. Chu, T.Y. Chen, W. Water, *J. Crystal Growth* 257 (2003) 280.
- [50] S. Muthukumar, C.R. Gorla, N.W. Emanetoglu, S. Liang, Y. Lu, *J. Crystal Growth* 225 (2001) 197.
- [51] C. Jagadish, S.J. Pearton, *Zinc Oxide Bulk, Thin Films and Nanostructures: Processing, Properties and Applications*, Elsevier, 2006.
- [52] K.S.A. Kumar, S.M. Chen, *Anal. Lett.* 41 (2008) 141–158.
- [53] K.B. Sundaram, A. Khan, *Thin Solid Films* 295 (1997) 87–91.
- [54] D.C. Look, D.C. Reynolds, C.W. Litton, R.L. Jones, D.B. Eason, G. Cantwell, *Appl. Phys. Lett.* 81 (2002) 1830.
- [55] M.N. Kamalasanan, S. Chandra, *Thin Solid Films* 288 (1996) 112–115.
- [56] S. Goldsmith, *Surf. Coat. Technol.* 201 (2006) 3993–3999.
- [57] W.L. Dang, Y.Q. Fu, J.K. Luo, A.J. Flewitt, W.I. Milne, *Superlattices Microstruct.* 42 (2007) 89–93.
- [58] O. Kluth, G. Schöpe, J. Hüpkes, C. Agashe, J. Müller, B. Rech, *Thin Solid Films* 442 (2003) 80.
- [59] V. Tvarozek, I. Novotny, P. Sutta, S. Flicyngerova, K. Schtereve, E. Vavrinsky, *Thin Solid Films* 515 (2007) 8756–8760.
- [60] S. Zhu, C. Su, S.L. Lehoczky, P. Peters, M.A. George, *J. Crystal Growth* 211 (2000) 106–110.
- [61] Ü. Özgür, Y.I. Alivov, C. Liu, et al., *J. Appl. Phys.* 98 (2005) 041301.
- [62] N. Fujimura, T. Nishihara, S. Goto, et al., *J. Crystal Growth* 130 (1993) 269.
- [63] M.H. Koch, A.J. Hartmann, R.N. Lamb, M. Neuber, M. Grunze, *J. Phys. Chem. B* 101 (1997) 8231–8236.
- [64] Y. Lee, Y. Kim, H. Kim, *J. Mater. Res.* 13 (1998) 1260–1265.
- [65] K. Chou, G. Liu, *J. Crystal Growth* 243 (2003) 439–443.
- [66] M. Kadoka, T. Miura, *Jpn. J. Appl. Phys.* 41 (2002) 3281.
- [67] T. Yanagitani, M. Matsukawa, Y. Watanabe, T. Otani, *J. Crystal Growth* 276 (2005) 424.
- [68] T. Yanagitani, S. Tomohiro, T. Nohara, et al., *Jpn. J. Appl. Phys.* 43 (2004) 3004.
- [69] M.H. Koch, A.J. Hartmann, R.N. Lamb, M. Neuber, M. Gruze, *J. Phys. Chem. B* 101 (1997) 8231.
- [70] Y. Yoshino, K. Lnoue, M. Takeuchi, T. Makino, Y. Katayama, T. Hata, *Vacuum* 59 (2000) 403–410.
- [71] E.K. Kim, T.Y. Lee, H.S. Hwang, et al., *Superlattice Microstruct.* 39 (2006) 138.
- [72] T. Matsuda, M. Furuta, T. Hiramatsu, et al., *J. Crystal Growth* 310 (2008) 31.
- [73] J.B. Lee, et al., *Thin Solid Films* 447–448 (2004) 296–301.
- [74] Y. Yoshino, *J. Appl. Phys.* 105 (2009) 061623.
- [75] J.P. Jung, J.B. Lee, J.S. Kim, J.S. Park, *Thin Solid Films* 444–448 (2004) 605–609.
- [76] Y.D. Jo, S.M. Koo, *Appl. Surf. Sci.* 255 (2009) 3480–3484.
- [77] M. Peruzzi, J.D. Pedarnig, D. Bauerle, W. Schwingger, F. Schaffler, *Appl. Phys. A* 79 (2004) 1873–1877.
- [78] R. Triboulet, J. Perriere, *Prog. Cryst. Growth Charact. Mater.* 47 (2003) 65–138.
- [79] T. Yanagitani, M. Kiuchi, *J. Appl. Phys.* 102 (2007) 044115.
- [80] T. Mitsuyu, S. Ono, K. Wasa, *J. Appl. Phys.* 51 (1980) 2464.
- [81] I. Petrov, V. Orlinov, A. Misiuk, *Thin Solid Films* 120 (1984) 55.
- [82] Y. Miyamoto, T. Yangaitani, Y. Watanabe, *Acoust. Sci. Technol.* 27 (2006) 53–55.
- [83] J.S. Wang, K.M. Lakin, *Appl. Phys. Lett.* 42 (1983) 352.
- [84] M. Link, M. Schreiter, J. Weber, R. Gabl, D. Pitzer, R. Primig, W. Wersing, M.B. Assouar, O. Elmazria, *J. Vac. Sci. Technol. A* 24 (2006) 218–222.
- [85] T. Lamara, M. Belmahi, O. Elmazria, L. Le Brizoul, J. Bougdira, M. Remy, P. Alnot, *Diamond Relat. Mater.* 13 (2004) 581–584.
- [86] M.E. Hakiki, O. Elmazria, P. Alnot, *IEEE Trans. Ultrason. Ferroelectr. Freq. Control* 54 (2007) 676–681.
- [87] V. Mortet, O.A. Williams, K. Haenen, *Phys. Stat. Sol.* 205 (2008) 1009–1020.
- [88] W.T. Lim, B.K. Son, D.H. Kang, C.H. Lee, *Thin Solid Films* 382 (2001) 56.

- [89] T. Lamara, M. Belmahi, O. Elmazria, L. Le Brizoual, J. Bougdira, M. Remy, P. Alnot, *Diamond Relat Mater.* 13 (2004) 581–584.
- [90] X.Y. Du, Y.Q. Fu, S.C. Tan, J.K. Luo, A.J. Flewitt, W.I. Milne, D.S. Lee, N.M. Park, J. Park, Y.J. Choi, S.H. Kim, S. Maeng, *Appl. Phys. Lett.* 93 (7) (2008) 094105.
- [91] B.A. Auld, *Acoustic Fields and Waves in Solids*, vol. II, John Wiley & Sons, New York, 1973, p. 319.
- [92] G.A. Armstrong, S. Crampm, *Electro. Lett.* 9 (1973) 322–323.
- [93] Y. Takagaki, P.V. Santos, E. Wiebicke, O. Bramdt, H.P. Schonheer, K.H. Ploog, *Appl. Phys. Lett.* 81 (2000) 14.
- [94] A. Talbi, F. Sarry, L.L. Brizoual, O. Elmazria, P. Alnot, *IEEE Trans. Ultrasonic Ferroelectr. Freq. Control* 51 (2004) 1421.
- [95] L. Le Brizoual, O. Elmazria, F. Sarry, M. El Hakiki, A. Talbi, P. Alnot, *Ultrasonics* 45 (2006) 100–103.
- [96] L. Le Brizoual, F. Sarry, O. Elmazria, P. Alnot, S. Ballandras, T. Patureaud, *IEEE Trans. Ultrasonic Ferroelectr. Freq. Control* 55 (2008) 442–450.
- [97] V.S. Pham, L. Mai, G. Yoon, *Jpn. J. Appl. Phys.* 47 (2008) 6383–6385.
- [98] Z. Yan, Z. Song, W. Liu, et al., *Appl. Surf. Sci.* 253 (2007) 9372–9380.
- [99] K.W. Tay, C.L. Huang, L. Wu, *Jpn. J. Appl. Phys.* 43 (3) (2004) 1122–1126.
- [100] E. Ntagwirumugra, T. Gryba, V.Y. Zhang, E. Dogheche, J.E. Lefebvre, *IEEE Trans. Ultrasonic Ferroelectr. Freq. Control* 54 (2007) 2011–2015.
- [101] M. Takeuchi, H. Yamada, Y. Yoshino, et al., *Vacuum* 66 (2002) 463–466.
- [102] Y. Yoshino, M. Takeuchi, K. Inoue, T. Makino, S. Arai, T. Hata, *Vacuum* 66 (2002) 467–472.
- [103] T. Xu, G. Wu, G. Zhang, Y. Hao, *Sens. Actuat. A* 104 (2003) 61.
- [104] J. Zhou, N. Xu, Z.L. Wang, *Adv. Mater.* 18 (2006) 2432.
- [105] H. Zheng, X.L. Du, Q. Luo, J.F. Jia, C.Z. Cu, Q.K. Xue, *Thin Solid Films* 515 (2007) 3969.
- [106] S.J. Pearton, D.P. Norton, K. Ip, Y.W. Heo, *J. Vac. Sci. Technol.* B22 (2004) 932.
- [107] R. Groenen, M. Creatore, M.C.M. Van de Sander, *Appl. Surf. Sci.* 241 (2005) 321–325.
- [108] S.R. Min, H.N. Cho, Y.L. Li, C.W. Chung, *Thin Solid Films* 516 (2008) 3521–3529.
- [109] G. Kenanakis, E. Stratakis, K. Vlachou, D. Vernardou, E. Koudoumas, N. Nat-sarakis, *Appl. Surf. Sci.* 254 (2008) 5695.
- [110] R.D. Sun, A. Nakajima, A. Fujishima, T. Watanabe, K. Hashimoto, *J. Phys. Chem. B* 105 (2001) 1984–1990.
- [111] X. Hou, F. Zhou, B. Yu, W. Liu, *Mater. Sci. Eng. A* 452–453 (2007) 732–736.
- [112] C. Badre, T. Pauporte, M. Turmine, D. Lincot, *Superlattices Microstruct.* 42 (2007) 99–103.
- [113] L. Mei, J. Zhai, H. Liu, Y. Song, L. Jiang, D. Zhu, *J. Phys. Chem. B* 107 (2003) 9954.
- [114] C.D. Corso, A. Dickherber, W.D. Hunt, *Biosens. Bioelectron.* 24 (2008) 805–811.
- [115] S. Krishnamoorthy, T. Bei, E. Zoumakis, G.P. Chrousos, A.A. Iliadis, *Biosens. Bioelectron.* 22 (2006) 707–714.
- [116] D.S. Lee, Y.Q. Fu, S. Maeng, J. Luo, N.M. Park, S.H. Kim, M.Y. Jung, W.I. Milne, ZnO surface acoustic wave biosensor, in: *International Electron Devices Meeting, Washington DC, December 10–12, 2007*.
- [117] S.Y. Chu, W. Water, J.T. Liaw, *Ultrasonics* 41 (2003) 133.
- [118] S.J. Jian, S.Y. Chu, T.Y. Huang, W. Water, *J. Vac. Sci. Technol.* A22 (2004) 2424–2430.
- [119] S. Krishnamoorthy, A.A. Iliadis, *Solid-State Electron.* 50 (2006) 1113.
- [120] G. Mchale, M.I. Newton, F. Martin, *J. Appl. Phys.* 91 (2002) 9701–9710.
- [121] D.A. Powell, K. Kalatair-Zadeh, W. Wlodaiski, *Sens. Actuat. A* 115 (2004) 456–461.
- [122] J. Du, G.L. Harding, *Sens. Actuat. A* 65 (1998) 152–159.
- [123] S. Wenzel, R. White, *Sens. Actuat. A* 21–23 (1990) 700.
- [124] R.M. White, *Faraday Discuss.* 107 (1997) 1.
- [125] I.Y. Huang, M.C. Lee, *Sens. Actuat. B* 132 (2008) 340–348.
- [126] J. Bjurström, D. Rosen, I. Katardjiev, V.M. Yanchev, I. Petrov, *IEEE Trans. Ultrasonic Ferroelectr. Freq. Control* 51 (2004) 1347.
- [127] Y.R. Kang, S.C. Kang, K.K. Paek, Y.K. Kim, S.W. Kim, B.K. Ju, *Sens. Actuat. A* 117 (2005) 62.
- [128] R. Gabl, H.D. Feucht, H. Zeininger, G. Eckstein, M. Schreter, R. Primig, D. Pitzer, W. Wersing, *Biosens. Bioelectron.* 19 (2004) 615.
- [129] R.C. Lin, Y.C. Chen, W.T. Chang, C.C. Cheng, K.S. Koo, *Sens. Actuat. A* 147 (2008) 425–429.
- [130] Z. Yan, X.Y. Zhu, G.K.H. Pang, *Appl. Phys. Lett.* 90 (2007) 143503.
- [131] M. Link, J. Webber, M. Schreiter, W. Wersing, O. Elmazria, P. Alnot, *Sens. Actuat. B* 121 (2007) 372.
- [132] J. Weber, W.M. Albers, J. Tuppurainen, M. Link, R. Gabl, W. Wersing, M. Schre-iter, *Sens. Actuat. A* 128 (2006) 84–88.
- [133] M. Link, M. Schreiter, J. Weber, R. Primig, D. Pitzer, R. Gabl, *IEEE Trans. Ultra-sonic Ferroelectr. Freq. Control* 53 (2006) 492–496.
- [134] Y.Q. Fu, X.Y. Du, J.K. Luo, A.J. Flewitt, M.I. Milne, *IEEE Trans. Ultrasonic Ferro-lectr. Freq. Control* (1–3) (2007) 478–483, 2008.
- [135] H. Nakamura, T. Yamada, T. Ishizaki, K. Nishimura, *IEEE Trans. Ultrasonic Ferroelectr. Freq. Control* 49 (2004) 761–768.
- [136] S. Lehtonen, V.P. Plessky, C.S. Hartmann, M. Salomaa, *IEEE Trans. Ultrasonic Ferroelectr. Freq. Control* 51 (2004) 1697–1703.
- [137] T.T. Wu, I.H. Chang, *J. Appl. Phys.* 98 (2005) 024903.
- [138] X.Y. Du, Y.Q. Fu, S.C. Tan, J.K. Luo, A.J. Flewitt, D.S. Lee, S. Maeng, S.H. Kim, Y.J. Choi, N.M. Park, J. Park, W.I. Milne, *J. Appl. Phys.* 105 (2009) 024508.
- [139] K. Chono, N. Shimizu, Y. Matui, Jun Kondoh, S. Shiokawa, *Jpn. J. Appl. Phys.* 43 (2004) 2987.
- [140] C.D. Wood, S.D. Evens, J.E. Cumingham, R. O'Rourke, C. Walti, A.G. Davies, *Appl. Phys. Lett.* 92 (2008) 044104.
- [141] H. Li, J.R. Friend, L.Y. Yeo, *Biomed. Microdev.* 9 (2007) 647.
- [142] R. Shilton, M.K. Tan, L.Y. Yeo, J.R. Friend, *J. Appl. Phys.* 104 (2008) 014910.
- [143] N.T. Nguyen, R.T. White, *Sens. Actuat.* 77 (1999) 229–236.
- [144] R.M. Moroney, R.M. White, R.T. Howe, *Appl. Phys. Lett.* 59 (1991) 774–776.
- [145] A.H. Meng, N.T. Nguyen, R.M. White, *Biomed. Microdev.* 2 (2000) 169–174.
- [146] X. Zhu, E.S. Kim, *Sens. Actuat. A* 66 (1998) 355–360.
- [147] P. Luginbuhl, S.D. Collins, G.A. Racine, M.A. Gretillat, N.F. De Rooij, K.G. Brooks, N. Setter, *J. MEMS* 6 (1997) 337–346.
- [148] J.W. Kwon, H. Yu, Q. Zou, E.S. Kim, *J. Micromech. Microeng.* 16 (2006) 2697–2704.
- [149] D. Huang, E. Kim, *J. MEMS* 10 (2001) 442–449.
- [150] J. Homola, S.S. Yee, G. Gauglitz, *Sens. Actuat. B* 54 (1999) 3–15.
- [151] S.S. Sokolowski, D.E. Trudell, J.E. Byrness, M. Okandan, J.M. Bauer, R.G. Manley, G.C. Freye-Mason, *IEEE Trans. Ultrasonic Ferroelectr. Freq. Control* 6 (2006) 784–795.
- [152] Li, W. Parkes, L.I. Haworth, A.W.S. Ross, J.T.M. Stevenson, A.J. Walton, *IEEE JMEMS* 17 (2008) 1481–1488.
- [153] R.B. Fair, *Microfluid Nanofluid* 3 (2007) 245–281.
- [154] Y. Li, B.W. Flynn, W. Parkes, et al., *ESSDERC (39th European Solid-State Device Research Conference)*, Athens, (2009) 371–374.
- [155] C.K. Lee, S. Cochran, A. Abrar, K.J. Kirk, F. Placido, *Ultrasonics* 42 (2004) 485–490.
- [156] G. Wingqvist, J. Bjurström, L. Liljeholm, et al., *Sens. Actuat. B* 123 (2007) 466–473.

Biographies

Richard Yongqing Fu received his Ph.D degree from Nanyang Technological University, Singapore in 1999. He worked as a research fellow and post-doc in the Nanyang Technological University, Singapore, Singapore-Massachusetts Institute of Technology Alliance and University of Cambridge. Starting from September 2007, he joined Heriot-Watt University in Edinburgh as a lecturer on microengineering and bio-engineering. His recent research work has focused on microactuators, biosensors, microfluidic devices and nanotechnology, based on smart functional materials and thin films (such as piezoelectric and shape memory thin films). He has authored and co-authored about 150 refereed international journal papers, one book on thin film shape memory alloys and ten book chapters in these areas. He has been regularly invited as referees for over 30 different international journals, and serves as editorial board member for three international journals.

Jack Luo received his Ph.D from the University of Hokkaido, Japan. He worked in Cardiff University, UK, Newport Wafer Fab. Ltd., Philips Semiconductor Co. and Cavendish Kinetics Ltd., Cambridge University. From January 2007, he became a Professor in MEMS at the Centre for Material Research and Innovation (CMRI), University of Bolton. His current research interests focus on microsystems and sensors for biotechnology and healthcare applications, and third generation thin film solar cells using novel low cost material.

Xiaoye Du graduated from University of Science and Technology in China. She obtained her Ph.D degree from University of Cambridge in 2009. Her research interests include MEMS, microfluidics, biosensor and Nanotechnology.

Andrew Flewitt, who is a member of Cambridge University Engineering Department, received his Ph.D from the University of Cambridge in 1998 investigating the growth of hydrogenated amorphous silicon thin films using scanning tunnelling microscopy. He stayed in the Engineering Department following the Ph.D. as a Research Associate sponsored by Philips Research Laboratories working on the low temperature fabrication of thin film transistors for liquid crystal displays. He was appointed to a Lectureship in August 2002, promoted to Senior Lecturer in 2006 and appointed Reader in Electronic Engineering in 2009. Current research interests include the degradation mechanisms of amorphous silicon thin films transistors, metal oxide thin film transistors, nanowire-polymer composite semiconductor materials and MEMS-based biological sensing devices using acoustic wave technology.

Yifan Li received B.S. degree in School of Electrical and Electronics, Shanghai Jiao Tong University, China in 2003, and his Ph.D in School of Engineering and Electronics, the University of Edinburgh, UK, 2007. He has been working in various MEMS areas in the past 5 years and now as a research associate. During his Ph.D study, he won the best presentation award in PREP2005 (IEEE & EPSRC). His current interest is microfluidic systems such as electro-wetting on dielectrics and surface acoustic wave, and bio-MEMS.

Gerard Markx is a Professor of Bioprocessing at Heriot-Watt University. His research interests include the use of microfabrication technology in biological systems and the 2D and 3D organisation of cells within films, aggregates and tissues, using a variety of cell culture, physical cell micromanipulation and cell immobilization techniques. He has strong expertise in the study of the dielectric properties of cells, and has pioneered the use of dielectrophoresis for the creation of cell aggregates with defined internal architectures, and its use for the study of cell-cell interactions.

Anthony J. Walton is professor of Microelectronic Manufacturing in the School of Engineering and Electronics at the University of Edinburgh. Over the past 25 years he has been actively involved with the semiconductor industry in a number of areas associated with silicon processing which includes both IC technology and micro-systems. In particular he has been intimately involved with the development of technologies and their integration with CMOS. He played a key role in setting up the

Scottish Microelectronics Centre (SMC) which is a purpose built facility for R&D and commercialisation. He has published over 300 papers and has won the best paper awards for the IEEE Transactions on Semiconductor Manufacturing, Proc ISHM, IEEE ICMTS 2004 as well as an IET Nanobiotechnology 2007 IET Premium Paper Award. He has served as the chairman for a number of conferences which include the European Solid-State Devices Research Conference (ESSDERC/CIRC 1994 and 2008) and the IEEE International Conference on Microelectronic Test Structures (ICMTS 1989 and 2008). He also serves on numerous technical committees and is an associate editor of the IEEE Transactions on Semiconductor Manufacturing and the Journal of Nanoengineering and Nanosystems.

Bill Milne (FREng) has been the Head of Electrical Engineering at Cambridge University since 1999, Director of the Centre for Advanced Photonics and Electronics (CAPE) since 2004 and Head of the Electronic Devices and Materials group since 1996

when he was appointed to the “1944 Chair in Electrical Engineering”. He obtained his BSc from St Andrews University in Scotland in 1970 and then obtained his Ph.D in Electronic Materials at Imperial College London in 1973 and a DIC. In 2003 he was awarded a D.Eng (Honoris Causa) from University of Waterloo, Canada. He was elected as Fellow of the Royal Academy of Engineering in 2006 and was awarded the JJ Thomson medal from the IET in 2008. He is a Guest Professor at HuangZhou University in Wuhan, China and a Distinguished Visiting Professor at SEU in Nanjing, China and at NUS, Singapore. He is also a Distinguished Visiting Scholar at KyungHee University, Seoul. His research interests include large area Si and carbon based electronics, thin film materials and, most recently, MEMS and carbon nanotubes and other 1D structures for electronic applications. He has published/presented about 650 papers, of which about 150 were invited.